Surface Science 668 (2018) 23–28

Contents lists available at ScienceDirect

Surface Science

journal homepage: www.elsevier.com/locate/susc

First principle study on the electronic properties and Schottky contact of graphene adsorbed on MoS_2 monolayer under applied out-plane strain

Huynh V. Phuc[a], Nguyen N. Hieu[a], Bui D. Hoi[b], Le T.T. Phuong[b], Chuong V. Nguyen[c,*]

[a] Institute of Research and Development, Duy Tan University, Da Nang, Viet Nam
[b] Department of Physics, University of Education, Hue University, Hue, Viet Nam
[c] Department of Materials Science and Engineering, Le Quy Don Technical University, Ha Noi, Viet Nam

ARTICLE INFO

Keywords:
Graphene
Electronic properties
Schottky contact
Out-plane strain
Heterointerface

ABSTRACT

In the present work, electronic properties and Schottky contact of graphene adsorbed on the MoS_2 monolayer under applied out-plane strain are studied using density functional theory calculations. Our calculations show that weak van derpp Waals interactions between graphene and monolayer MoS_2 are dominated at the interlayer distance of 3.34 Å and the binding energy per C atom of −25.1 meV. A narrow band gap of 3.6 meV has opened in G/MoS_2 heterointerface, and it can be modulated by the out-plane strain. Furthermore, the Schottky barrier and Schottky contact types in the G/MoS_2 heterointerface can be controlled by the out-plane strain. At the equilibrium state (d = 3.34 Å), the intrinsic electronic structure of G/MoS_2 heterointerface is well preserved and forms an n-type Schottky barrier of 0.49 eV. When the interlayer distance decreases, the transition from n-type to p-type Schottky contact occurs at d = 2.74 Å. Our studies promote the application of ultrathin G/MoS_2 heterointerface in the next-generation nanoelectronic and photonic devices such as van-der-Waals-based field effect transistors.

1. Introduction

Graphene is two-dimensional (2D) material with one-atom thickness and high carrier mobility [1,2]. However, graphene is a gapless semiconductor that causes the biggest problem for applications to graphene-based electronic devices [3,4]. Furthermore, electronic properties of graphene are very sensitive to external conditions such as impurities [5,6], external electric field [7] and interaction between graphene and substrates [7,8]. There exist several ways to open the band gap of graphene. One of them is mixing or hybridization the electronic states at K and K' by breaking the translational symmetry at Dirac point of π and π^* energy bands. An other way is breaking the sublattice symmetry in graphene. A simple way to control and modulate the band gap of graphene is deposition of the graphene on a substrate. Moreover, it is clear that the substrates are an essential component in graphene-based electronic devices.

The weak van-der-Waals (vdW) interaction between graphene and 2D semiconductor substrates has also been widely studied both theoretically and experimentally in several systems, such as G/MoS_2 [9], G/SiC [10], G/h-BN [8,11], G/α-Al_2O_3 [12], and G/P [13]. Varchon and co-workers studied the possibility of opening a band gap at the Dirac point in the system of graphene deposited on SiC substrate [14]. Besides, the effect of the substrate on electronic properties of graphene has been investigated experimentally [15]. G. Giovannetti *et. al* shown that the graphene/h-BN heterointerface has a band gap of 53 meV [8]. It means that the band gap at the Dirac points of graphene is effectively modulated by the interaction with the h-BN substrate. Moreover, Huang's group has demonstrated that the graphene became a semiconductor with a band gap of about 180 meV when it locates on the Al_2O_3 substrate [16]. Recently, the interaction between graphene and MoS_2 monolayer has also been studied theoretically [9,17,31]. In addition, the G/MoS_2 interface was successfully synthesized experimentally [18–20].

It is noted that MoS_2 monolayer is a semiconductor with a direct band gap of 1.80 eV [21,22]. The band gap is opened between the lowest energy of the conduction band and the highest energy of the valence band at the K-point. Moreover, MoS_2 monolayer has been successfully fabricated [23] and widely studied both experimentally [21,24] and theoretically [25–29] due to its extraordinary properties, for example, high on/off current ratio of about 10^8 [30], and high room-temperature carrier mobility of 200 cm^2/Vs [30]. These characters make MoS_2 monolayers a promising material for applications in nanoelectronic and optoelectronic devices.

Interestingly, metal/semiconductor interface, such as G/MoS_2 interface, is a new contact type of the graphene-based vdW interfaces. This vdW interface shows much more novel properties than their unique

* Corresponding author.
E-mail addresses: chnguyen@donstu.ru, chuongnguyen11@gmail.com (C.V. Nguyen).

https://doi.org/10.1016/j.susc.2017.10.011
Received 13 September 2017; Received in revised form 9 October 2017; Accepted 11 October 2017
Available online 12 October 2017
0039-6028/

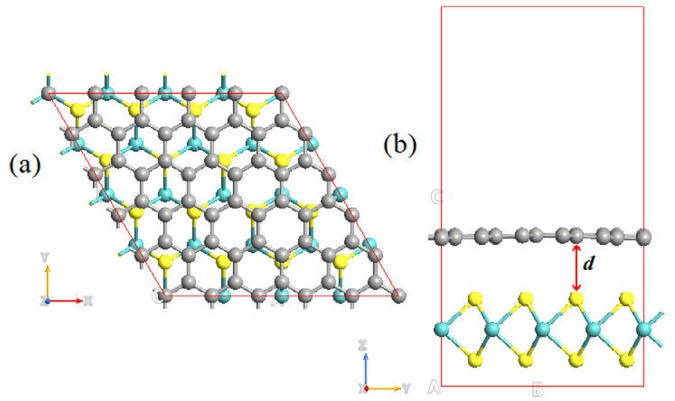

Fig. 1. Atomic structure of G/MoS_2. Top (a), side (b) views of relaxed atomic structure of G/MoS_2 interface. d is the interlayer distance between graphene and MoS_2. The blue, violet, and yellow balls stand for Mo, S, and C atoms, respectively. (For interpretation of the references to color in this figure legend, the reader is referred to the web version of this article.)

structures and the Schottky contact can be formed at the G/MoS_2 interface. Also, it can be controlled by an external electric field and in-plane strain [31–33]. Liu and co-workers showed that the Schottky barrier of G/MoS_2 heterointerface depends linearly on the electric field intensity [31]. In another work, they showed that the Schottky barrier can be controlled by the vertical electric field at the G/antimonene interface [32].

In this work, we investigate the electronic properties of the interaction between graphene and MoS_2 monolayer (G/MoS_2 interface) using first-principles calculations with vdW correction. The interaction between graphene and MoS_2 monolayer is described by a weak vdW interaction at the equilibrium state. The dependence of band structures of G/MoS_2 interface on the interlayer distances and the formation of Schottky contact at the G/MoS_2 interface have also investigated. Moreover, the coupling between layers can be used to effectively control the Schottky barrier (*n*-type and *p*-type). Our results may prove some applications in vdW-based field effect transistors (FETs).

2. Computational model and method

Our DFT calculations are performed using the plane wave basic as implemented in Quantum Espresso simulation package [34]. The ion-electron interaction is described by using the projector-augmented plane wave (PAW) approximation. The generalized gradient approximation (GGA) with the Perdew–Burke–Ernzerhof (PBE) functional is used for geometry optimization. The cut-off energy of 500 eV is adopted in our calculations. The Brillouin zone was represented by Monkhorst-Pack mesh of $(9\times9\times1)$ is used for electronic band structure. It is known that the weak interactions are out of the framework of standard PBE functional. Thus we add the DFT-D2 (where D stands for dispersion) method with the Grimme vdW correction [35] to describe the weak interactions. Previously, we have used successfully this method for calculations of layered materials, such as graphene nanoribbon, MoS_2 or graphene placed on semiconductor substrates [36–40].

The scheme of G/MoS_2 interface is shown in Fig. 1. The lattice parameters of the pristine graphene and the MoS_2 monolayer are 2.46 Å and 3.18 Å, respectively, which are in good agreement with the previous theoretical and experimental results [22,36,41,42]. Thus, we choose MoS_2 monolayer as a substrate to match well with graphene. We also use a supercell, which consists (5 × 5) unit cells of graphene and (4 × 4) unit cells of MoS_2 monolayer along the x and y directions. The lattice mismatch between graphene and MoS_2 monolayer, therefore, is only about 2 %. A vacuum space of 22 Å in the z direction is used to avoid the interaction between neighbor slabs.

The binding energy per carbon atom between graphene and MoS_2 monolayer is calculated by $E_b = -[E_{G/MoS_2} - (E_G + E_{MoS_2})]/N_C$, where E_{G/MoS_2}, E_G, and E_{MoS_2} are the total energy of the G/MoS_2 interface, freestanding graphene, and isolated MoS_2 monolayer, respectively. N_C is the number of carbon atoms in the supercell.

3. Results and discussion

Firstly, we calculate the electronic band structures of freestanding graphene and MoS_2 monolayer in the supercells using DFT-D2 calculations, as shown in Fig. 2(a and b). Our calculations show that the freestanding graphene has zero-gap [Fig. 2(a)] and monolayer MoS_2 is a semiconductor with a direct band gap of 1.70 eV [Fig. 2(b)]. These results are in good agreement with those obtained in previous theoretical work [43]. We now investigate the electronic properties of the interface between graphene and monolayer MoS_2 (G/MoS_2) after full relaxation. It is noted that the lattice mismatch between graphene and MoS_2 monolayer is small, about 2%. This small lattice mismatch has little affects on their electronic properties, and thus it does not affect the main results.

To obtain the equilibrium state, the G/MoS_2 interface is relaxed by using the DFT-D2 method. The relaxed atomic structure of G/MoS_2 interface is shown in Fig. 1. At equilibrium state, the interlayer distance between graphene and MoS_2 layers is $d_0 = 3.34$ Å and the binding energy per carbon atom in G/MoS_2 interface is $E_b = -25.1$ meV. These values are close to the previous theoretical and experimental results in graphene/substrate interface [8,44–46]. The negatible binding energy implies that the interaction between graphene and MoS_2 monolayer is a weak vdW and electrostatic interactions.

The electronic band structure of the G/MoS_2 interface is shown in Fig. 2(c). We can see that the linear Dirac-like dispersion relation near the Fermi level of graphene is still preserved in G/MoS_2 interface. Magnifying the linear band structure, we can see that a band gap in G/MoS_2 interface is opened at the Dirac K-point of graphene [see the inset in Fig. 2(c)]. It means that at the Dirac K-point, the π and π^* bands repulse each other, forming a small energy band gap. Therefore, the G/MoS_2 interface is a semiconductor with a narrow direct energy gap, describing the effect of MoS_2 substrate on the electronic properties of graphene. Thus, the MoS_2 substrate can be used as an ideal substrate for graphene-based devices. The opened band gap of G/MoS_2 interface, as shown in the inset in Fig. 2(c), is 3.6 meV. This gap is smaller than that of G/*h*-BN [8,47,48], G/ZnO [46,49], and G/P [13,50,51]. To understand the physical nature of the band gap opening in G/MoS_2 interface, we use the tight-binding (TB) model analysis. According to the π-electron TB approximation of graphene, the dispersion relation near the Fermi level can be approximated as:

$$E(k) = \pm\sqrt{\Delta^2 + (\hbar v_F k)^2}$$

where k is the wave vector relative to Dirac point, v_F is the Fermi velocity, and Δ is the on-site energy difference between the two sub-lattices of graphene. The signs correspond to conduction bands and valence bands, respectively. For freestanding graphene monolayer, the onsite energies of the two sub-lattices are identical ($\Delta = 0$), resulting in the zero band gap and the linear dispersion relation near the Dirac point. For the G/MoS_2 heterointerface, the charge redistribution breaks the equivalence of the two graphene sub-lattices, giving rise to a non zero band gap, $E_g = 2\Delta$.

We now investigate the effect of out of plane strain on the electronic property of G/MoS_2 interface. The out of plane strain is applied by changing the interlayer distance as $\varepsilon = (d - d_0)/d_0$, where d and d_0 are the interlayer distances under applied strain and at equilibrium state, respectively. The interlayer distance varies from 2.44 Å to 4.24 Å along the z-direction. It means that the out of plane strain varies from −27% to 27%. In Fig. 3 we show the band structures of G/MoS_2 interface at different interlayer distances. We can see that with increasing the interlayer distance, the conduction bands at Dirac point move downward to the Fermi energy level, whereas the valence bands shift downward

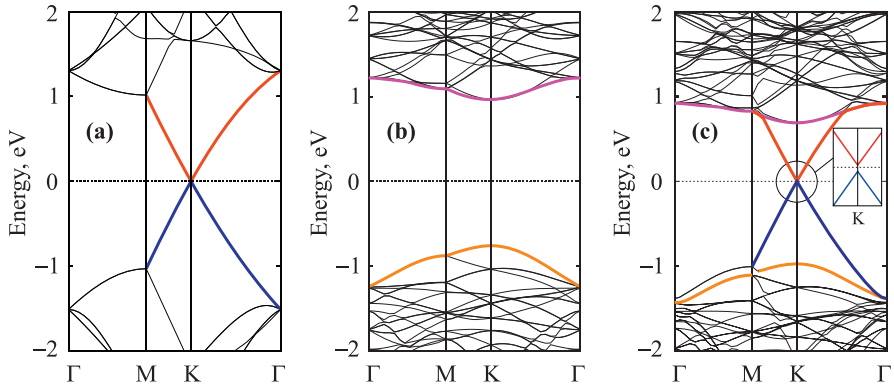

Fig. 2. DFT-D2 calculations of the band structure of freestanding graphene (a), substrate MoS_2 (b), and coupling G/MoS_2 interface (c). The blue, and red lines stand respectively for bonding π-band and antibonding π^*-band of graphene. The purple, and orange lines stand for the conduction band minimum and the valence band maximum of isolated MoS_2 monolayer, respectively. (For interpretation of the references to color in this figure legend, the reader is referred to the web version of this article.)

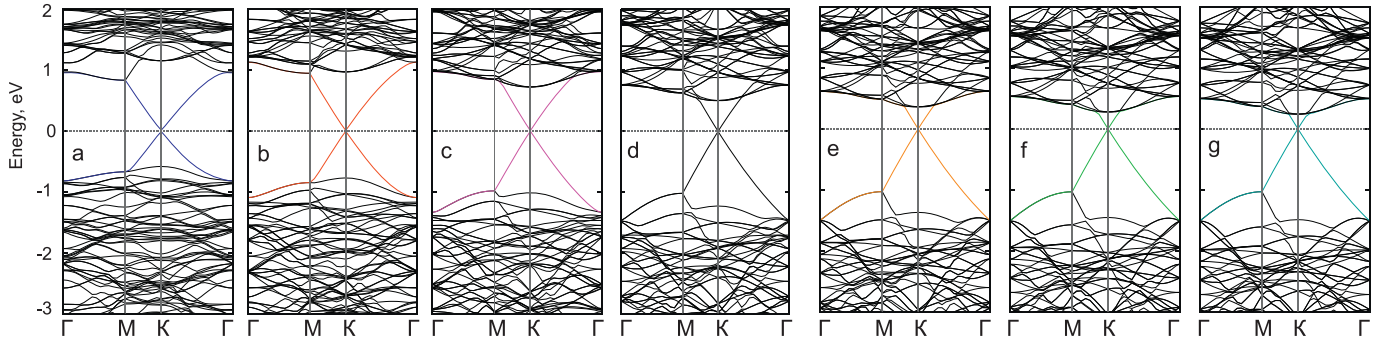

Fig. 3. Electronic energy band structure of G/MoS_2 interface with different interlayer distances d: (a) d = 2.44 Å, (b) d = 2.74 Å, (c) d = 3.04 Å, (d) d = 3.34 Å, (e) d = 3.64 Å, (f) d = 3.94 Å, and (g) d = 4.24 Å.

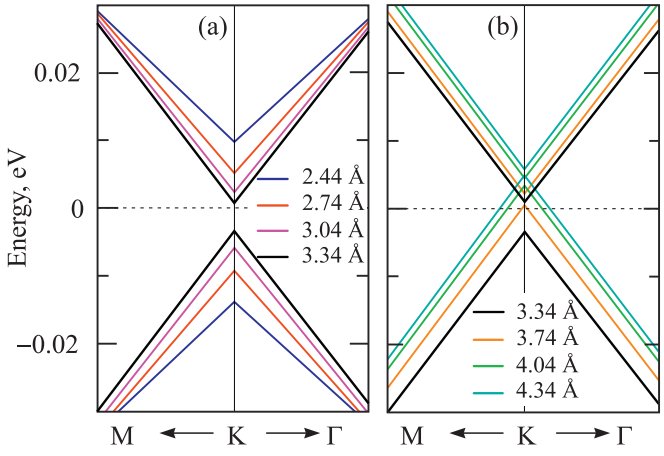

Fig. 4. Linear dispersion near the Fermi level at Dirac point of G/MoS_2 interface at the different interlayer distances d: (a) $d \le d_0$, (b) $d \ge d_0$.

from Fermi energy level. However, in all case of interlayer distances, the Dirac cone always locates at the *K*-point. It can be concluded that the electronic structure around the Dirac cone of graphene is almost not affected by the interlayer distance.

To describe the effect of the interlayer distance on the band gap of G/MoS_2 interface, in Fig. 4 we show the energy dispersion near the Fermi energy level at Dirac point for the valence band maximum (VBM) and the conduction band minimum (CBM) in the band structures of G/MoS_2 interface at different interlayer distances. In the case of $d > d_0$, when the interlayer distance increases, the bonding π-bands tend to go up to the Fermi level [see Fig. 4(b)]. The effect of the interlayer distance on the band gap and total energy is shown in Fig. 5. We can see that, at a large interface distance $d \ge 3.74$ Å, the Dirac point of graphene moves up to the Fermi level, leading to the *p*-type (hole) doping in graphene in the graphene/MoS_2 interface, as shown in Fig. 4(b). As shown in Fig. 5(a), the total energy of G/MoS_2 interface is minimum at the equilibrium state of d_0 = 3.34 Å. Therefore, it can be concluded that the band gap of graphene/MoS_2 interface depends strongly on the interlayer distance, especially when $d < d_0$.

Interestingly, in this interface, we found a Schottky contact, which has been formed between the metallic graphene and the semiconducting MoS_2 substrate. Our calculations show that the Schottky barrier can be controlled by the interlayer distance between the layers. We show the dependence of the Schottky barrier on the interlayer distance in Fig. 6. Based on the Schottky–Mott model [52] at the metal/semiconductor interface [53], the *n*-type Schottky barrier is defined by $\Phi_{B,n} = E_C - E_F$, where E_C is the conduction band minimum (CBM) and E_F is the Fermi energy level, respectively. The *p*-type Schottky barrier is defined by $\Phi_{B,p} = E_V - E_F$, where E_V is the valence band maximum (VBM). Note that the sum of the *n*-type and *p*-type Schottky barrier is approximately equal to the band gap of the semiconductor, that is $\Phi_{Bn} + \Phi_{Bp} \approx E_g(MoS_2)$. At the equilibrium state, the Fermi level locates at the middle of the band gap between the CBM and VBM bands. In Fig. 6, we plot the evolution of the *n*-type Φ_{Bn} and *p*-type Φ_{Bp} Schottky contact. It can be seen that the system at the equilibrium state shows an *n*-type Schottky contact with the barrier of $\Phi_{B,n}$ = 0.49 eV. With increasing the interlayer distance to d = 4.24 Å (ε = 27%), the system still preserves *n*-type Schottky contact. The Schottky barrier decreases from 0.49 eV down to 0.28 eV and to 0.24 eV with the increasing distance from 3.34 Å (ε = 0%) to 3.94 Å (ε = 18%) and to 4.24 Å (ε = 27%), respectively. This behavior can be explained as follows: when the interlayer distance increases, chemical interactions in the G/MoS_2 interface becomes weaker, resulting in

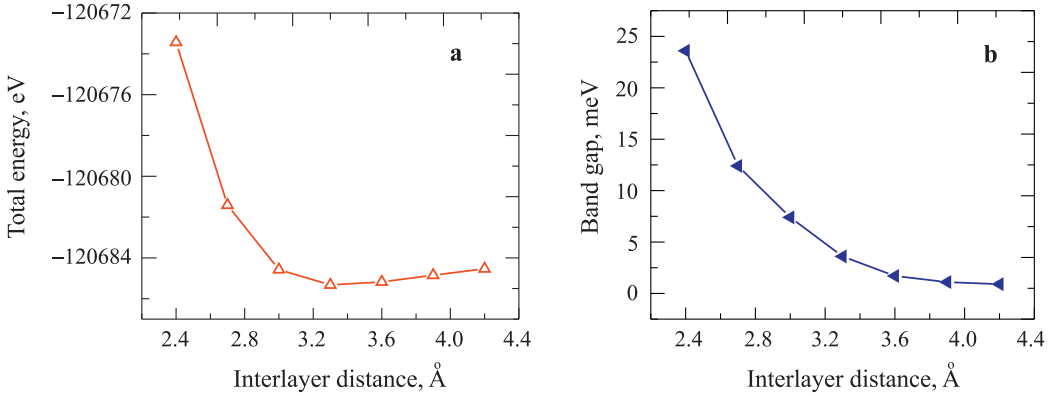

Fig. 5. Dependence of the total energy (a) and band gap (b) of G/MoS_2 interface on the interlayer distance.

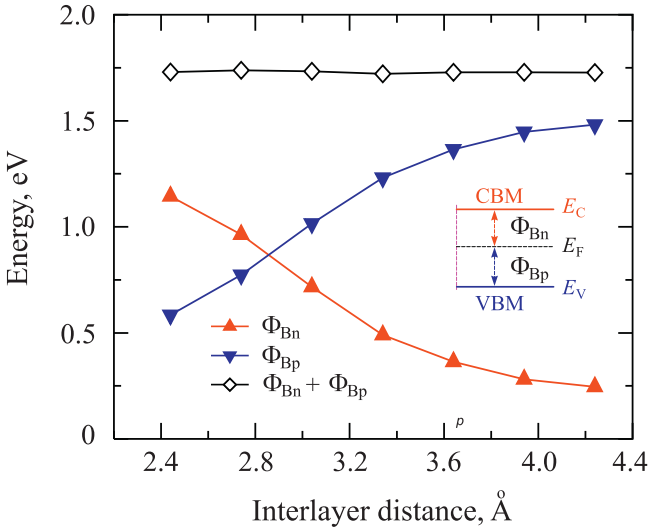

Fig. 6. Dependence of the Schottky barrier in G/MoS_2 interface on the interlayer distance.

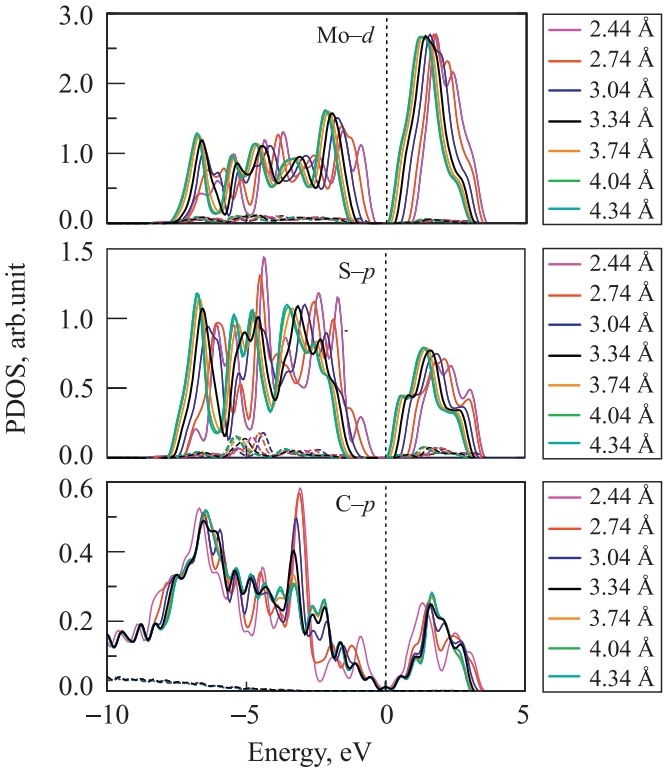

Fig. 7. Partial density of states (PDOS) of Mo-*d* (a), S-*p* (b) and C-*p* (c) orbitals in the G/MoS_2 systems with different interlayer distances.

fewer electrons transfer from MoS_2 to graphene. With the decrease of the interlayer distance to 3.04 Å ($\varepsilon = -9\%$), the system shows a *n*-type Schottky contact with the barrier height of $\Phi_{B,n} = 0.72$ eV. However, when the interlayer distance decreases to 2.74 Å ($\varepsilon = -18\%$) and 2.44 Å ($\varepsilon = -27\%$), the Schottky barrier is transformed from *n*-type to *p*-type Schottky contact. The transition of the Schottky barrier is located at the interlayer distance of 2.74 Å with the Schottky barrier of $\Phi_{B,p} = 0.77$ eV. The Schottky barrier $\Phi_{B,p}$ decreases to 0.51 eV at the interlayer distance of 2.44 Å. Thus, the interlayer distance not only controls the Schottky barrier but also causes the Schottky barrier transition from *n*-type to *p*-type Schottky contact.

It is clear that the G/MoS_2 interface becomes an unified electronic system as the contact between graphene and MoS_2 monolayer, resulting in the appearance of a small band bending. The band bending can be defined as $\Delta W = W_{G/MoS_2} - W_{MoS_2}$, where W_{G/MoS_2} is the work function of the G/MoS_2 interface and W_{MoS_2} is the work function of the isolated MoS_2 monolayer. The calculated work function of the G/MoS_2 interface and isolated MoS_2 monolayer at the equilibrium state is 4.80 eV and 4.92 eV, respectively. Thus, the band bending at the equilibrium state is only −0.12 eV, which implies a n-type Schottky contact in the G/MoS_2 interface. By increasing the interlayer distance *d* from 3.34 Å to 4.24 Å, the work function of the G/MoS_2 interface decreases from 4.80 eV to 4.70 eV, respectively, resulting in a decrease of the band bending from −0.12 eV to −0.22 eV, respectively. In contrast, by decreasing the interlayer distance the band bending increases. For example, the band bending is 4.91 eV and 4.95 eV at the interlayer distance of 3.04 Å and 2.74 Å, respectively. It can be seen that at the interlayer distance of 2.74 Å, the band bending is greater than zero ($\Delta W = 0.03$ eV), which presents a p-type Schottky contact.

To have a more explicit view of the effect of the interlayer distance on the electronic properties of G/MoS_2 interface, we plot the partial density of states (PDOS) for the C-p_z, Mo-*d*, and S-*p* orbitals in the interface, as shown in Fig. 6. It shows that the G/MoS_2 interface is a semiconductor at the equilibrium state with the Fermi level located between the VBM and the CBM. Both the VBM and the CBM are formed by the C-*p*, S-*p* and Mo-*d* states. By changing the interlayer distance between graphene and MoS_2 monolayer, the S-*p* and Mo-*d* states are upshifted or/and downshifted, as shown in Fig. 7. With increasing the interlayer distance from 3.34 Å to 4.24 Å, the semiconductor-metal transition has been observed due to existence of the VBM at the Fermi level.

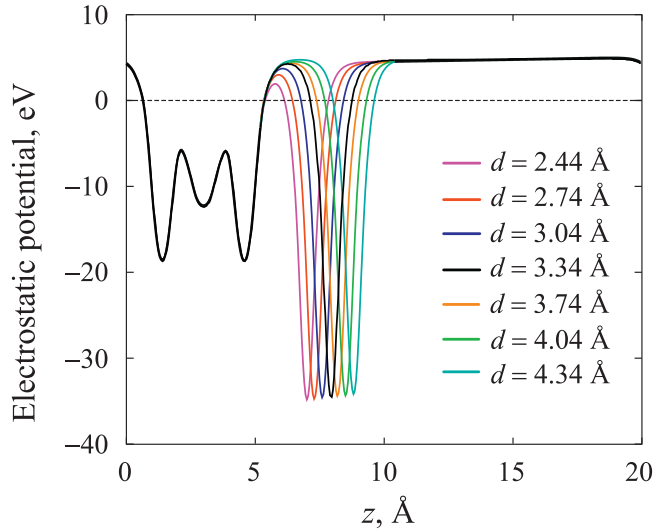

Fig. 8. The electrostatic potentials of G/MoS_2 interface at different interlayer distances d along z-direction. Note that the MoS_2 layer in interface is fixed and only the graphene layer is moved away from the MoS_2 layer.

Fig. 8 shows the electrostatic potential of G/MoS_2 interface along the z-direction at different interlayer distances. We found that the energy level of graphene is downshifted to the valence band of MoS_2 with decreasing the interlayer distance from 4.24 Å to 2.44 Å. Our work function of freestanding graphene of 4.4 eV is in good agreement with the experimental data of 4.514 eV [54]. Also, the work function of MoS_2 monolayer is 4.9 eV. The transition from n-type to p-type Schottky contact at $d = 2.74$ Å can be explained by the transfer of electrons from MoS_2 to graphene layer. It indicates that the electrons are likely to move into graphene layer by decreasing the interlayer distance. It also can be seen from Fig. 8, the vdW interaction at $d = 4.24$ Å is weak and the effect of graphene on MoS_2 and vice versa is negligible. In this case, the electrostatic potential well of MoS_2 is much higher than that of graphene. When the interlayer distance decreases, the tunneling energy barrier at interface gradually shifts downward so that more electrons get favored to transfer from MoS_2 layer to graphene.

4. Conclusion

In conclusion, the electronic properties of G/MoS_2 interface have been studied using density functional theory with added vdW correction method. Our calculations show that at the equilibrium state, the interlayer distance between graphene and MoS_2 substrate is $d_0 = 3.34$ Å and thus it is characterized by the vdW interaction with the binding energy per carbon atom of −25.1 meV. In the presence of MoS_2 substrate, graphene has a small band gap of 3.6 meV. This band gap depends strongly on the interlayer distance d when $d < d_0$. At the equilibrium state, the graphene/MoS_2 interface has n-type Schottky contact with the Schottky barrier $\Phi_{Bn} = 0.49$ eV. The transition from n-type to p-type Schottky contact can be observed at $d = 2.74$ Å. Our results indicate that the G/MoS_2 interface can be used in electronic and optoelectronic devices, such as the field effect transistors.

Acknowledgments

This research is funded by Vietnam National Foundation for Science and Technology Development (NAFOSTED) under Grant number 103.01-2016.07.

References

[1] K.S. Novoselov, A.K. Geim, S.V. Morozov, D. Jiang, Y. Zhang, S.V. Dubonos, I.V. Grigorieva, A.A. Firsov, Electric field effect in atomically thin carbon films, Science 306 (5696) (2004) 666–669. http://science.sciencemag.org/content/306/5696/666.
[2] A.K. Geim, K.S. Novoselov, The rise of graphene, Nat. Mater. 6 (3) (2007) 183–191. https://www.nature.com/nmat/journal/v6/n3/full/nmat1849.html.
[3] S.Y. Zhou, G.-H. Gweon, A. Fedorov, P. First, W. De Heer, D.H. Lee, F. Guinea, A.C. Neto, A. Lanzara, Substrate-induced bandgap opening in epitaxial graphene, Nat. Mater. 6 (10) (2007) 770–775.
[4] Y. Zhang, T.T. Tang, C. Girit, Z. Hao, M.C. Martin, A. Zettl, M.F. Crommie, Y.R. Shen, F. Wang, Direct observation of a widely tunable bandgap in bilayer graphene, Nature 459 (7248) (2009) 820–823.
[5] A. Katanin, Effect of weak impurities on electronic properties of graphene: Functional renormalization-group analysis, Phys. Rev. B 88 (24) (2013). 241401–. https://link.aps.org/doi/10.1103/PhysRevB.88.241401..
[6] J. Zhang, W. Xie, X. Xu, S. Zhang, J. Zhao, Structural and electronic properties of interfaces in graphene and hexagonal boron nitride lateral heterostructures, Chem. Mater. 28 (14) (2016) 5022–5028.
[7] K. Chen, X. Wang, J.-B. Xu, L. Pan, X. Wang, Y. Shi, Electronic properties of graphene altered by substrate surface chemistry and externally applied electric field, J. Phys. Chem. C 116 (10) (2012) 6259–6267.
[8] G. Giovannetti, P.A. Khomyakov, G. Brocks, P.J. Kelly, J. van den Brink, Substrate-induced band gap in graphene on hexagonal boron nitride: Ab initio density functional calculations, Phys. Rev. B 76 (2007) 073103, doi:10.1103/PhysRevB.76.073103.
[9] W. Hu, T. Wang, R. Zhang, J. Yang, Effects of interlayer coupling and electric fields on the electronic structures of graphene and MoS_2 heterobilayers, J. Mater. Chem. C 4 (9) (2016) 1776–1781. http://pubs.rsc.org/-/content/articlehtml/2016/tc/c6tc00207b.
[10] A. Mattausch, O. Pankratov, Ab initio study of graphene on SiC, Phys. Rev. Lett. 99 (7) (2007) 076802. https://journals.aps.org/prl/abstract/10.1103/PhysRevLett.99.076802.
[11] R. Balu, X. Zhong, R. Pandey, S.P. Karna, Effect of electric field on the band structure of graphene/boron nitride and boron nitride/boron nitride bilayers, Appl. Phys. Lett. 100 (5) (2012) 052104. http://aip.scitation.org/doi/abs/10.1063/1.3679174.
[12] B. Huang, Q. Xu, S.H. Wei, Theoretical study of corundum as an ideal gate dielectric material for graphene transistors, Phys. Rev. B 84 (15) (2011) 155406. https://journals.aps.org/prb/abstract/10.1103/PhysRevB.84.155406.
[13] W. Hu, T. Wang, J. Yang, Tunable schottky contacts in hybrid graphene–phosphorene nanocomposites, J. Mater. Chem. C 3 (18) (2015) 4756–4761. http://pubs.rsc.org/-/content/articlehtml/2015/tc/c5tc00759c.
[14] F. Varchon, R. Feng, J. Hass, X. Li, B.N. Nguyen, C. Naud, P. Mallet, J.-Y. Veuillen, C. Berger, E.H. Conrad, L. Magaud, Electronic structure of epitaxial graphene layers on sic: Effect of the substrate, Phys. Rev. Lett. 99 (2007) 126805, doi:10.1103/PhysRevLett.99.126805.
[15] L. Magaud, F. Hiebel, F. Varchon, P. Mallet, J.-Y. Veuillen, How the sic substrate impacts graphene's atomic and electronic structure, Phys. Stat. Sol. (RRL) 3 (6) (2009) 172–174. https://doi.org/10.1002/pssr.200903145.
[16] B. Huang, Q. Xu, S.H. Wei, Theoretical study of corundum as an ideal gate dielectric material for graphene transistors, Phys. Rev. B 84 (15) (2011) 155406.
[17] N.N. Hieu, H.V. Phuc, V.V. Ilyasov, N.D. Chien, N.A. Poklonski, N.V. Hieu, C.V. Nguyen, First-principles study of the structural and electronic properties of graphene/mos2 interfaces, J. Appl. Phys. 122 (10) (2017) 104301.
[18] K. Chang, W. Chen, l-cysteine-assisted synthesis of layered MoS_2/graphene composites with excellent electrochemical performances for lithium ion batteries, ACS Nano 5 (6) (2011) 4720–4728, doi:10.1021/nn200659w.
[19] J.N. Coleman, M. Lotya, A. O'Neill, S.D. Bergin, P.J. King, U. Khan, K. Young, A. Gaucher, S. De, R.J. Smith, I.V. Shvets, S.K. Arora, G. Stanton, H.-Y. Kim, K. Lee, G.T. Kim, G.S. Duesberg, T. Hallam, J.J. Boland, J.J. Wang, J.F. Donegan, J.C. Grunlan, G. Moriarty, A. Shmeliov, R.J. Nicholls, J.M. Perkins, E.M. Grieveson, K. Theuwissen, D.W. McComb, P.D. Nellist, V. Nicolosi, Two-dimensional nanosheets produced by liquid exfoliation of layered materials, Science 331 (6017) (2011) 568. http://science.sciencemag.org/content/331/6017/568.abstract.
[20] Y. Li, H. Wang, L. Xie, Y. Liang, G. Hong, H. Dai, MoS_2 nanoparticles grown on graphene: An advanced catalyst for the hydrogen evolution reaction, J. Am. Chem. Soc. 133 (19) (2011) 7296–7299, doi:10.1021/ja201269b.
[21] K.F. Mak, C. Lee, J. Hone, J. Shan, T.F. Heinz, Atomically thin MoS_2: A new direct-gap semiconductor, Phys. Rev. Lett. 105 (2010) 136805, doi:10.1103/PhysRevLett.105.136805.
[22] C.V. Nguyen, N.N. Hieu, Effect of biaxial strain and external electric field on electronic properties of MoS_2 monolayer: A first-principle study, Chem. Phys. 468 (2016) 9–14.
[23] D. Kim, D. Sun, W. Lu, Z. Cheng, Y. Zhu, D. Le, T.S. Rahman, L. Bartels, Toward the growth of an aligned single-layer MoS_2 film, Langmuir 27 (18) (2011) 11650–11653, doi:10.1021/la201878f.
[24] S.W. Han, H. Kwon, S.K. Kim, S. Ryu, W.S. Yun, D.H. Kim, J.H. Hwang, J.-S. Kang, J. Baik, H.J. Shin, S.C. Hong, Band-gap transition induced by interlayer van der waals interaction in MoS_2, Phys. Rev. B 84 (2011) 045409, doi:10.1103/PhysRevB.84.045409.
[25] C. Ataca, M. Topsakal, E. Akturk, S. Ciraci, A comparative study of lattice dynamics of three-and two-dimensional MoS_2, J. Phys. Chem. C 115 (33) (2011) 16354–16361. http://pubs.acs.org/doi/abs/10.1021/jp205116x.
[26] S. Lebègue, O. Eriksson, Electronic structure of two-dimensional crystals from ab initio theory, Phys. Rev. B 79 (2009) 115409, doi:10.1103/PhysRevB.79.115409.

[27] S. Yu, H.D. Xiong, K. Eshun, H. Yuan, Q. Li, Phase transition, effective mass and carrier mobility of mos 2 monolayer under tensile strain, Appl. Surface Sci. 325 (2015) 27–32.
[28] D. Ma, W. Ju, T. Li, X. Zhang, C. He, B. Ma, Y. Tang, Z. Lu, Z. Yang, Modulating electronic, magnetic and chemical properties of mos 2 monolayer sheets by substitutional doping with transition metals, Appl. Surface Sci. 364 (2016) 181–189.
[29] D. Ma, W. Ju, T. Li, X. Zhang, C. He, B. Ma, Z. Lu, Z. Yang, The adsorption of co and no on the mos 2 monolayer doped with au, pt, pd, or ni: A first-principles study, Appl. Surface Sci. 383 (2016) 98–105.
[30] B. Radisavljevic, A. Radenovic, J. Brivio, i.V. Giacometti, A. Kis, Single-layer mos2 transistors, Nature Nanotechnol. 6 (3) (2011) 147–150. http://www.nature.com/nnano/journal/v6/n3/abs/nnano.2010.279.html.
[31] X. Liu, Z. Li, Electric field and strain effect on graphene-MoS_2 hybrid structure: ab initio calculations, J. Phys. Chem. Lett. 6 (16) (2015) 3269–3275.
[32] W. Li, X. Wang, X. Dai, Tunable schottky contacts in the antimonene/graphene van der waals heterostructures, Solid State Commun. 254 (2017) 37–41.
[33] W. Xiong, C. Xia, X. Zhao, T. Wang, Y. Jia, Effects of strain and electric field on electronic structures and schottky barrier in graphene and SnS hybrid heterostructures, Carbon 109 (2016) 737–746.
[34] P. Giannozzi, S. Baroni, N. Bonini, M. Calandra, R. Car, C. Cavazzoni, D. Ceresoli, G.L. Chiarotti, M. Cococcioni, I. Dabo, A.D. Corso, S. de Gironcoli, S. Fabris, G. Fratesi, R. Gebauer, U. Gerstmann, C. Gougoussis, A. Kokalj, M. Lazzeri, L. Martin-Samos, N. Marzari, F. Mauri, R. Mazzarello, S. Paolini, A. Pasquarello, L. Paulatto, C. Sbraccia, S. Scandolo, G. Sclauzero, A.P. Seitsonen, A. Smogunov, P. Umari, R.M. Wentzcovitch, QUANTUM ESPRESSO: A modular and open-source software project for quantum simulations of materials, J. Phys 21 (39) (2009) 395502. http://stacks.iop.org/0953-8984/21/i=39/a=395502..
[35] S. Grimme, Semiempirical GGA-type density functional constructed with a long-range dispersion correction, J. Comput. Chem. 27 (15) (2006) 1787–1799, doi:10.1002/jcc.20495.
[36] C.V. Nguyen, N.N. Hieu, D.T. Nguyen, Dispersion-corrected density functional theory investigations of structural and electronic properties of bulk MoS_2: Effect of uniaxial strain, Nanoscale Res. Lett. 10 (1) (2015) 433. https://nanoscalereslett.springeropen.com/articles/10.1186/s11671-015-1099-5.
[37] C.V. Nguyen, N.N. Hieu, V.V. Ilyasov, Band gap modulation of bilayer MoS_2 under strain engineering and electric field: A density functional theory, J. Electr. Mater. 45 (8) (2016) 4038–4043, doi:10.1007/s11664-016-4593-3.
[38] V.V. Ilyasov, C.V. Nguyen, I.V. Ershov, N.N. Hieu, Electric field and substrate-induced modulation of spin-polarized transport in graphene nanoribbons on a3b5 semiconductors, J. Appl. Phys. 117 (17) (2015) 174309, doi:10.1063/1.4919920.
[39] V.V. Ilyasov, I.G. Popova, I.V. Ershov, N.D. Chien, N.N. Hieu, C.V. Nguyen, First principles study of structural, electronic and magnetic properties of graphene adsorbed on the o-terminated mno(111) surface, Diamond Relat. Mater. 74 (2017) 31–40. http://www.sciencedirect.com/science/article/pii/S0925963516307269.
[40] V.V. Ilyasov, B. Meshi, I. Popova, I.V. Ershov, N.N. Hieu, C.V. Nguyen, First-principles study of the structural and electronic properties of graphene absorbed on mno(1 1 1) surfaces, Comput. Theor. Chem. 1098 (2016) 22–30. http://www.sciencedirect.com/science/article/pii/S2210271X16304315.
[41] A.K. Geim, K.S. Novoselov, The rise of graphene, Nat. Mater. 6 (3) (2007) 183–191.
[42] J. Wilson, A. Yoffe, The transition metal dichalcogenides discussion and interpretation of the observed optical, electrical and structural properties, Adv. Phys. 18 (73) (1969) 193–335.
[43] H. Ramakrishna Matte, A. Gomathi, A.K. Manna, D.J. Late, R. Datta, S.K. Pati, C. Rao, MoS_2 and WS_2 analogues of graphene, Angewandte Chemie 122 (24) (2010) 4153–4156.
[44] S. Entani, L.Y. Antipina, P.V. Avramov, M. Ohtomo, Y. Matsumoto, N. Hirao, I. Shimoyama, H. Naramoto, Y. Baba, P.B. Sorokin, et al., Contracted interlayer distance in graphene/sapphire heterostructure, Nano Res. 8 (5) (2015) 1535–1545.
[45] B. Liu, L.-J. Wu, Y.-Q. Zhao, L.-Z. Wang, M.-Q. Cai, First-principles investigation of the schottky contact for the two-dimensional MoS_2 and graphene heterostructure, RSC Adv. 6 (65) (2016) 60271–60276.
[46] P. Xu, Q. Tang, Z. Zhou, Structural and electronic properties of graphene–ZnO interfaces: dispersion-corrected density functional theory investigations, Nanotechnology 24 (30) (2013) 305401.
[47] C.R. Dean, A.F. Young, I. Meric, C. Lee, L. Wang, S. Sorgenfrei, K. Watanabe, T. Taniguchi, P. Kim, K.L. Shepard, et al., Boron nitride substrates for high-quality graphene electronics, Nat. Nanotechnol. 5 (10) (2010) 722–726.
[48] J. Xue, J. Sanchez-Yamagishi, D. Bulmash, P. Jacquod, A. Deshpande, K. Watanabe, T. Taniguchi, P. Jarillo-Herrero, B.J. LeRoy, Scanning tunnelling microscopy and spectroscopy of ultra-flat graphene on hexagonal boron nitride, Nat. Mater. 10 (4) (2011) 282–285.
[49] T. Kavitha, A.I. Gopalan, K.-P. Lee, S.-Y. Park, Glucose sensing, photocatalytic and antibacterial properties of graphene–ZnO nanoparticle hybrids, Carbon 50 (8) (2012) 2994–3000.
[50] Y. Cai, G. Zhang, Y.-W. Zhang, Electronic properties of phosphorene/graphene and phosphorene/hexagonal boron nitride heterostructures, J. Phys. Chem. C 119 (24) (2015) 13929–13936.
[51] L.-M. Liu, First-principles study of phosphorene and graphene heterostructure as anode materials for rechargeable Li batteries, J. Phys. Chem. Lett.s 6 (2015) 5002–5008.
[52] J. Bardeen, Surface states and rectification at a metal semi-conductor contact, Phys. Rev. 71 (1947) 717–727.
[53] W. Chen, E.J. Santos, W. Zhu, E. Kaxiras, Z. Zhang, Tuning the electronic and chemical properties of monolayer MoS_2 adsorbed on transition metal substrates, Nano Lett. 13 (2) (2013) 509–514.
[54] S.-J. Liang, L. Ang, Electron thermionic emission from graphene and a thermionic energy converter, Phys. Rev. Appl. 3 (1) (2015) 014002.